Chaos

Wavelet skeletons in sleep EEG-monitoring as biomarkers of early diagnostics of mild cognitive impairment

Cite as: Chaos **31**, 073110 (2021); https://doi.org/10.1063/5.0055441
Submitted: 29 April 2021 . Accepted: 15 June 2021 . Published Online: 02 July 2021

Konstantin Sergeev, Anastasiya Runnova, Maksim Zhuravlev, Oleg Kolokolov, Nataliya Akimova, Anton Kiselev, Anastasiya Titova, Andrei Slepnev, Nadezhda Semenova, and Thomas Penzel

COLLECTIONS

Paper published as part of the special topic on In Memory of Vadim S. Anishchenko: Statistical Physics and Nonlinear Dynamics of Complex Systems

Wavelet skeletons in sleep EEG-monitoring as biomarkers of early diagnostics of mild cognitive impairment

Cite as: Chaos **31**, 073110 (2021); doi: 10.1063/5.0055441
Submitted: 29 April 2021 · Accepted: 15 June 2021 ·
Published Online: 2 July 2021

Konstantin Sergeev,[1] Anastasiya Runnova,[1,2,a)] Maksim Zhuravlev,[1,2] Oleg Kolokolov,[2] Nataliya Akimova,[2] Anton Kiselev,[2,3] Anastasiya Titova,[2] Andrei Slepnev,[1] Nadezhda Semenova,[1,4] and Thomas Penzel[1,5]

AFFILIATIONS

[1]Saratov State University, Astrakhanskaya Str., 83, Saratov 410012, Russia
[2]Saratov State Medical University, B. Kazachaya Str., 112, Saratov 410012, Russia
[3]National Medical Research Center for Therapy and Preventive Medicine, 10, Petroverigsky per., Moscow 101953, Russia
[4]FEMTO-ST Institut, Université Bourgogne Franche-Comté, 15B avenue des Montboucons, Besançon Cedex 25030, France
[5]Charité—Universitätsmedizin Berlin, Charitéplatz 1, 10117 Berlin, Germany

Note: This paper is part of the Focus Issue, In Memory of Vadim S. Anishchenko: Statistical Physics and Nonlinear Dynamics of Complex Systems.

[a)]**Author to whom correspondence should be addressed:** runnova.ae@staff.sgmu.ru

ABSTRACT

Many neuro-degenerative diseases are difficult to diagnose in their early stages. For example, early diagnosis of Mild Cognitive Impairment (MCI) requires a wide variety of tests to distinguish MCI symptoms and normal consequences of aging. In this article, we use the wavelet–skeleton approach to find some characteristic patterns in the electroencephalograms (EEGs) of healthy adult patients and patients with cognitive dysfunctions. We analyze the EEG activity recorded during natural sleep of 11 elderly patients aged between 60 and 75, six of whom have mild cognitive impairment, and apply a nonlinear analysis method based on continuous wavelet transformskeletons. Our studies show that a comprehensive analysis of EEG signals of the entire sleep state allows us to identify a significant decrease in the average duration of oscillatory patterns in the frequency band [12; 14] Hz in the presence of mild cognitive impairment. Thus, the changes in this frequency range can be interpreted as related to the activity in the motor cortex, as a candidate for developing the criteria for early objective MCI.

The study presented in the article is aimed at developing methods for early objective diagnosis of mild cognitive impairment (MCI) in humans. Today, with the continuous growth of life expectancy in developed countries, the problem of identifying biomarkers of changes in normal cognitive aging is very acute in psychiatry and neurology. Early detection of such biomarkers would allow starting treatment of such conditions before the moments of pronounced clinical symptoms and signs of disease. The article discusses the change in the characteristics of the brain activity of such patients during a night's sleep. This approach to the analysis of EEG signals can be considered as an additional study, for example, with polysomnographic control, and serve as an independent objective marker for assessing the risks of cognitive impairment.

I. INTRODUCTION

An analysis of biological data using methods of nonlinear dynamics may reveal information on the functional state of living systems. A huge amount of information about the organism's state can be derived from the electrical signals that accompany the processes in heart and brain functions. Recently, a lot of diagnostic techniques based on this approach were developed, but the task of diagnosing (especially early diagnosis) various diseases has not yet been completely accomplished.

It is especially difficult to diagnose various neurodegenerative diseases. Neuro-degenerative diseases [Alzheimer's disease (AD) and other forms of dementia] are dangerous diseases that significantly reduce the quality of life and increase mortality. There are five

stages of AD.[1] The first stage, known as Mild Cognitive Impairment (MCI), is usually accompanied by memory loss and does not significantly affect daily life.[2,3] The second stage involves forgetfulness, short-term memory loss, repetitive questions, and loss of hobbies and interests, resulting in limitations in the activities of daily living limitations. The third stage represents the progression of cognitive deficits, dysexecutive syndrome, further impaired activities of daily living, transitions in care, and emergence of behavioral and psychological symptoms of dementia. The fourth stage leads to agitation, altered sleep patterns, and establishment of behavioral and psychological symptoms of dementia; the patients need assistance in dressing, feeding, and bathing. The last stage ends in bedbound, no speech, incontinence, and a loss of basic psychomotor skills.

Stages two to five are fairly easy to identify by their obvious symptoms. But the diagnosis of MCI is a complicated task because it is difficult to distinguish MCI symptoms and normal consequences of aging. A disease-modifying effect correlated with a persistent delay in the underlying pathological process is difficult to prove without validated biomarkers.[4,5] The diagnosis requires a wide variety of tests, including a psychological test, blood and spinal fluid tests, and neurological examination.[6–10] Moreover, in the last few years, many groups have started exploring the use of biomedical signals, such as EEG, near-infrared spectroscopy (NIRS activity, its typical applications include medical and physiological diagnostics and research including blood sugar, pulse oximetry, functional neuroimaging, etc.), and others for early diagnosis of AD. Today, the most common method for the registration of brain activity is electroencephalography, being the cheapest and simple safe technology widely used in clinical practice.

From the physical point of view, EEG realization is a complex non-stationary signal generated by the cerebral cortex nerve cells. Depending on where the signal was taken from, there are two types of EEG: scalp (non-invasive) and intracranial (invasive). In the case of scalp EEG, small metal electrodes are placed on the scalp with good mechanical and electrical contact. Intracranial EEG is obtained by implanting special electrodes implanted in the brain during a surgery. The changes in the voltage difference between low-impedance (<5 kOhm) electrodes are sensed and amplified before being transmitted to a computer program to display the tracing of voltage potential recordings.[11]

EEG signals contain a wide range of frequency components in between 0.1 and 70 Hz. This range can be roughly divided into the following frequency bands: Delta (<4 Hz), Theta (4–8 Hz), Alpha (8–12 Hz), Beta1 (12–24 Hz), Beta2 (24–30 Hz), and Gamma (>30 Hz).[12] During different types of cognitive activity and/or physiological state, EEG signals show an increased oscillatory energy in different frequency bands. However, a flexible separation of oscillatory activity in narrow bands, tuned for different study tasks, is often used.

It has been shown that AD has (at least) three major effects on EEG: 1, slowing of the EEG [increase in power in the low-frequency range (Delta and Theta) and decrease in power in the high-frequency range (Alpha and Beta)]; 2, an enhanced complexity of the EEG signals; and 3, perturbations in EEG synchrony.[13,14] These effects, however, are not always easily detectable because of a large variability among AD patients. Moreover, none of those phenomena allow at present to reliably diagnose AD at an early stage.[13]

Historically, an analysis of EEG includes the examination of the following features: frequency (or wavelength); voltage (or amplitude); wave-form regularity; and reactivity to eye opening, hyperventilation, and photonic stimulation through visual inspection,[15] various types of evoked potentials,[16,17] and Fourier analysis.[18,19] The quantitative analysis based on the Fourier approach allows us to determine averaged frequency composition over a finite time interval, but it does not make possible to consider how the frequency composition of the signal changes in time. Therefore, other methods for analyzing non-stationary complex signals developed and applied in nonlinear dynamics are well applicable, such as time-series analysis,[20,21] spatiotemporal analysis,[22] network approaches,[23] etc. In addition, today, applied methods of EEG processing based on artificial neural networks and machine learning occupy a significant niche of applied problems such as signal artifact filtration,[24,25] automatic detection of special events,[26–29] BCI modules,[30,31] etc.

The group of Vadim Semenovich Anishchenko was actively involved in the study of biological signals using approaches that are typical of chaos theory, such as Lyapunov analysis,[32] multifractal dimension estimation,[33] synchronization theory,[34,35] and others.[36–40]

Many research groups use the wavelet analysis for exploring EEGs. This approach has found application in a wide range of tasks related to the EEG analysis[41–43] (e.g., epilepsy research[44,45] and sleep staging[46,47]). The wavelet analysis is the main tool for processing EEG data in real time and creating brain–computer interface (BCI) devices.[42,48,49] The main advantage of the wavelet approach is that it provides the ability to perform multiscale signal analysis and, in consequence, the possibility of performing the time–frequency sweep of non-stationary signals. This allows us to see the interaction of events on a small scale, growing into large-scale phenomena.

In the presented work, we use the wavelet–skeleton approach to find some characteristic patterns in the EEGs of healthy adult patients and patients with cognitive dysfunctions. We try to avoid strong individual variability in the dynamics of brain activity by examining the state of the night sleep of patients. Then the total number of patterns and their averaged durations are compared for healthy and unhealthy patients. In some frequency diapason, the difference between durations of patterns is large enough to recognize the MCI.

II. MATERIALS AND METHODS

A. Data and materials

The participants volunteered in our clinical trial on a complimentary basis. All study subjects signed an informed consent to participate in the clinical trial, received all necessary explanations about the research, and agreed to the subsequent publication of study results. Collected experimental data were processed with respect to confidentiality and anonymity of research participants. The design of the clinical trial was approved by the local research Ethics Committee. The clinical trial subjects were recruited from the patients at the University clinical hospital named after S. R. Mirotvortsev (Saratov, Russian Federation).

The inclusion criteria for our study were as follows:

- written informed consent obtained before any assessment is performed as part of the study;

- male or female, age 60–75 years inclusive, females must be considered post-menopausal;
- psychological readiness to receive information, participant has evidence of adequate functioning relating to cognition and ability to communicate;
- no complaints for insufficient and nonrestorative sleep; and
- no sleep onset disorder (<30 min to fall asleep, no more one awakening per night of >15 min) per last 6 months.

The exclusion criteria were as follows:

- any disability that may prevent the participants from completing all study requirements (e.g., blindness, deafness, and severe language difficulty);
- Beck Depression Inventory score (BDI) > 13 (BDI is a 21-question multiple-choice self-report inventory, one of the most widely used psychometric tests for measuring the severity of depression. 0–9 points indicate minimal depression, whereas 30–63 points indicate severe depression);
- a score of >7 on the Hospital Anxiety and Depression Scale (HADS, it is commonly used by doctors to determine the levels of anxiety and depression that a person is experiencing. Each of the seven questions is scored from 0 to 3 and this means that a person can score between 0 and 21 for either anxiety or depression);
- an apnea–hypopnea index [AHI, an index used to indicate the severity of sleep apnea (pauses in breathing during sleep) where the normal state corresponds to AHI < 5 and severe sleep apnea corresponds to AHI > 30] and/or periodic limb movements index (PLM) > 5 and/or restless leg syndrome (RLS, a long-term disorder that causes a strong urge to move one's legs) during the polysomnography night;
- current medical or neurological condition that might impact cognition or performance on cognitive assessments (e.g., dementia, Huntington's disease, Parkinson's disease, Lyme disease, schizophrenia, bipolar disorder, major depression, active seizure disorder, history of multiple traumatic brain injuries, alcohol/drug abuse or dependence currently, or dependence within the last two years); and
- advanced, severe progressive, or unstable disease that may interfere with safety, tolerability, and study assessments or put the participant at special risk [e.g., active hepatitis, HIV infection, severe renal impairment, severe hepatic impairment, uncontrolled or significant cardiac disease including recent (within 6 months) myocardial infarction, congestive heart failure (functional class III–IV), or unstable angina].

A sleep diary was kept daily for a week by every participant. All patients underwent neuropsychological status assessment by means of the Montreal Cognitive Assessment [MoCA, 10-min cognitive screening tool to assist first-line physicians in the detection of mild cognitive impairment (MCI), a clinical state that often progresses to dementia];[50] Hospital Anxiety and Depression Scale (HADS); somnolence and sleep quality test; and tests for semantic and phonemic awareness and memory. The sleep interviews and medical examination were conducted by the physicians, certified in neurology and sleep medicine, whereas the psychiatric interviews were conducted by board-certified psychiatrists.

A comparative assessment of the cognitive functions in study participants via MoCA revealed a significant difference in indicators according to which the patients were divided into two groups. The first group included patients with MoCA scores of ≤27, and the second group included patients with MoCA scores of >27.

The first group included six patients with MCI caused by normal cognitive aging and/or dementia (group I, $n = 6$; BMI: $34.2 \pm 3.8\,\mathrm{kg/m^2}$; BDI: 8.5 ± 3.5; HADS: 7 ± 1; MoCA 25.5 ± 1.5). The second control group comprised five patients (group II, $n = 5$; BMI: $20.3 \pm 1.2\,\mathrm{kg/m^2}$; BDI: 8 ± 4; HADS: 7 ± 2; MoCA 28.5 ± 0.5). An average age of the subjects was 67 years 7 months.

The experiments were carried out in the late afternoon hours at a specially equipped polysomnographic laboratory. The laboratory was a comfortable, soundproofed room. Patients came to the clinic in the evening with their usual night clothes. After the necessary standard preparation of the equipment, the patient fell asleep at a convenient time.

The multichannel surface EEG data were collected using the Encephalan-EEGR-19/26 recorder (Medicom MTD Ltd, Russia). Data were recorded at 250 Hz sampling rate using the conventional monopolar method of registration with two referential points and N = 31 electrodes located in the 10–10 scheme[51] [see Fig. 1(a)]. The adhesive Ag/AgCl electrodes in prewired head caps were used to obtain the EEG signals. Two reference electrodes, A1 and A2, were located on mastoids, while the ground electrode N was placed above the forehead. The EEG signals were filtered by a bandpass filter with cutoff points at 0.5 Hz (HP) and 70 Hz (LP) and a 50 Hz notch filter. We performed a numerical analysis of the EEG signals recorded during the patient's nocturnal sleep—from the moment of falling asleep to the moment of full awakening, followed by morning rise.

B. Time–frequency analysis

In order to detect the oscillatory patterns in complex non-stationary signals based on the continuous wavelet transform (CWT),[52–54]

$$W(s,t) = \sqrt{s}\int_{-\infty}^{\infty} x(t)\psi^*\left(\frac{t-t_0}{s}\right)dt, \tag{1}$$

where $x(t)$ is the analyzed signal, s is the time scale that determines the wavelet width, "*" is the complex conjugation, and $\psi_{t_0,s}(t)$ is the basis of the wavelet transform in the form of a complex function. In the framework of working with biological signals, the Morlet wavelet[54] is traditionally used as the basis function,

$$\psi_{t_0,s}(t) = \sqrt{f}\pi^{\frac{1}{4}}\, e^{j\omega_0 f(t-t_0)}\, e^{\frac{f(t-t_0)^2}{2}}, \tag{2}$$

where $\omega_0 = 2\pi$ is the wavelet scaling parameter that provides a relationship between the time scale of the wavelet transform (s) and the Fourier transform frequency (f), where $f = 1/s$. Thus, using the Morlet wavelet basis, we can work with the usual classical frequency representation of signals when calculating CWT.

The main advantages of the wavelet analysis are the simplicity of the time–frequency sweep of noisy non-stationary signals and the good speed of numerical processing. Using CWT makes it possible to clearly and accurately trace the dynamics of the dominant components with a maximum frequency in the signal. However, when

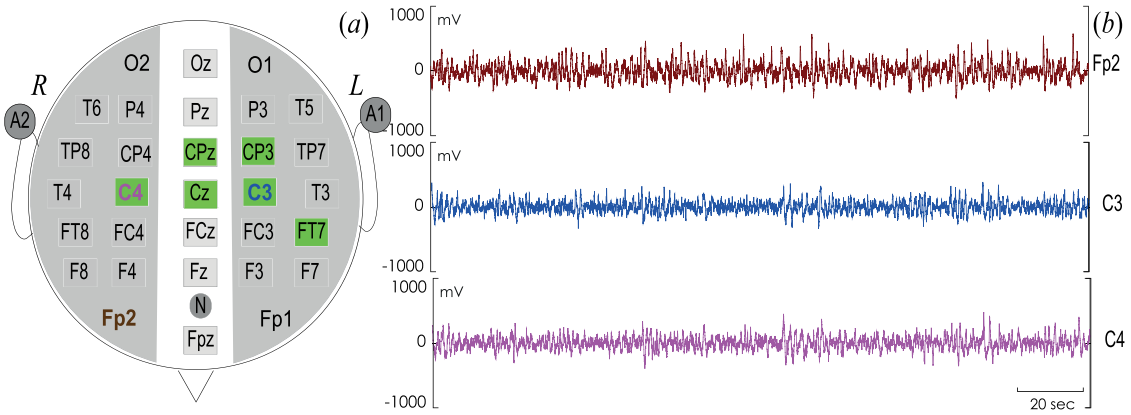

FIG. 1. (a) The scheme of the standard "10–10" electrodes layout. Different background colors, gray and white, correspond to left, right, and center scalp spatial zones, respectively. (b) Fragments of EEG signals recorded during the experimental active stage. The signals are shown in colors according to the corresponding recording electrodes.

considering the dynamics in the accompanying frequency ranges, one faces a problem of identifying the various patterns of activity that exist at the same time in the original complex signals. In biological systems like neural ensembles, it seems that different patterns of activity can simultaneously develop.[55,56] Even in model systems, coupled neural ensembles demonstrate the presence of several synchronous modes that switch when the nature of the connection changes.[57,58] Apparently, in the study of recorded brain activity, we can observe similar processes, which, however, are very difficult to detect. A simple assessment of the presence and the amount of oscillatory activity in different frequency ranges substantially aggravates the situation and, possibly, complicates the task of assessing the dynamics of processes actually occurring in a biological system, for example, reducing the quality of work of neurointerface devices.

The skeleton CWT method[53,59,60] is used to improve the quality of assessment of such coexisting processes. This technique is based on the identification of local maximum in the instantaneous distribution of CWT energy in the analyzed frequency range at any time. The following relation determines the instant CWT-energy distribution:

$$E(f, t_n) = \left|W(f, t_n)\right|^2. \tag{3}$$

For each moment t_n, there is a set of frequencies f_i with $i = 1, 2, \ldots, k$, where each skeleton is observed at frequency f_i, i.e., the local maximum amplitude of instantaneous energy CWT (3). In this processing, we consider all set $f_i|_{i=1..N}$ without ranking by the amplitude value of the instantaneous energy $E(f, t_n)$. The sequence number i characterizes only the sequence number of the extrema and is not related to the amplitude $E(f_i, t_n)$. Thus, in the process of analyzing the total duration of the studied signal, a set of frequencies f_i^n is formed, where n is the duration of the experimental signal, i.e., the number of time samples in the signal.

Next, we denote the condition for the development of an activity pattern with frequency f_j. To do this, we consider the following condition on each time interval $[t_n; t_{n+1}]$ for each frequency f_j:

$$\left|f_j^n - f_s^{n+1}\right| < \delta, \tag{4}$$

where f_j^n are sets of frequencies for which local maximum $E(f_j, t_n)$ (3) is at time step t_n, f_j^{n+1} are similar sets of frequencies with local maximum $E(f_j, t_{n+1})$ for the next time step t_{n+1}, and δ is the numerical constant based on the characteristics of the experimental signal. The choice of δ value in (4) was due to the used sampling steps at frequencies f and, accordingly, time scales s in the numerical implementation of the continuous wavelet transform. For this task, the step $\Delta s = 0.02$ was used. As empirical estimates have shown, δ should not exceed double Δs and $\delta = 0.04$ in all calculations.

If the condition (4) holds for some frequencies $f_{(a1)^n}$ and $f_{(a2)^{n+1}}$, then these frequencies are used in the development of one oscillatory pattern in time interval $[t_n; t_{n+1}]$. We now denote the frequency data $f_{(a1)^n}$ and $f_{(a2)^{n+1}}$ as $(a1)$ and $(a2)$, respectively. Next, for frequency $(a2)$, we again analyze (4) for the next time step t_{n+2}. If the condition also holds for the new time step, then the identified pattern will continue further with a certain frequency $(a3)$.

The described actions must be cyclically repeated until the condition (4) becomes not fulfilled, in other words, until the end of the activity of this oscillatory pattern. Thus, each oscillatory pattern P can be described by the frequency at each time moment of its existence, i.e., $P(f, t) = \{\{(a1), t_n\}, \{(a2), t_{n+1}\}, \ldots, \{(am), t_{n+m}\}\}$, where m characterizes the time duration of pattern's "life." Then the time duration of pattern P can be defined as

$$\tau = t_{n+m} - t_n, \tag{5}$$

and for the case of equidistant experimental time series, we use the expression $\tau = m\Delta t$, where Δt is the sampling time interval in the experimental series. So, the average frequency f_{md} can be estimated for each frequency pattern P as

$$f_{md} = \sum_{i=1}^{m} (ai)/m. \tag{6}$$

For further analysis, we denote the following selection criterion for correct oscillatory patterns P. If the time duration τ of the pattern P does not exceed the oscillation period of its average frequency

f_{md}, i.e., $\tau < (f_{md})^{-1}$, then this pattern must be considered as random noise interference and should not be taken into account in the further analysis of the signal.

We divide the entire significant frequency range of the EEG signal into 10 intervals: Δf_1 [1; 2,5] Hz, Δf_2 [2,5; 4,5] Hz, Δf_3 [4,5; 6,5] Hz, Δf_4 [5; 9] Hz, Δf_5 [9; 12] Hz, Δf_6 [12; 14] Hz, Δf_7 [14; 20] Hz, Δf_8 [20; 30] Hz, Δf_9 [7; 9] Hz, and Δf_{10} [6; 9] Hz. For the analysis of psychophysiological states and cognitive processes, standard frequency ranges are usually considered—delta, theta, alpha, beta, and gamma. However, today it is often even in neuropsychiatric research, for example, that the alpha and beta ranges are divided into 1–3 intervals. In addition, for example, in Ref. 61 demonstrated that the results of evaluations of oscillatory modes in various neurological disorders are typically only 2.2 times as likely to occur in the literature as alternate results and typically with less than 250 study participants when summed across all studies reporting this result. Moreover, as rightly described in meta-review,[61] there is often some confusion when describing the standard frequency ranges. While alpha and theta were more consistent, delta could start anywhere from 0 to 2 Hz and end anywhere from 3.5 to 6 Hz. Meanwhile, beta could begin anywhere between 12 and 15 Hz and end anywhere between 20 and 50 Hz. Across all bands, the most frequently used range was found in only 30%–50% of studies depending on the particular band. What one publication means by ≪delta≫ or ≪beta≫ (etc.) is therefore not necessarily the same as what another publication means by the same terminology. Thus, although in our work, we analyzed the oscillation activity in independent frequency intervals, we can compare with a certain accuracy the selected intervals to the traditional ones, namely, Δf_2 corresponds to delta band, Δf_4 similar to theta, Δf_5 similar to alpha, and Δf_7 and Δf_8 similar to beta 1 and beta 2 correspondingly. After that, for each frequency interval Δf, we estimate the time-normalized number of $N_{\Delta f}$ patterns with an average frequency f_{md} falling in this frequency interval Δf, namely,

$$N_{\Delta f} = \frac{m}{t_2 - t_1} \text{ for } \forall P, \text{ if } f_{md} \in \Delta f, \tag{7}$$

where m is the total number of oscillatory patterns P and t_1 and t_2 are the start and end recording time.

Also, for each episode of wakefulness/sleep, we calculate the average normalized time length of the "life," the duration $T_{\Delta f}$ of the pattern is calculated according to the following equation:

$$T_{\Delta f} = \frac{\sum_{k=1}^{m} \tau_k}{t_2 - t_1} \text{ for } \forall P, \text{ if } f_{md} \in \Delta f, \tag{8}$$

where τ_k is the time duration of the kth oscillatory pattern with an average frequency f_{md} lying within the boundaries of a certain frequency range Δf during a recording time.

III. RESULTS

As a result of EEG data processing, we have obtained a lot of information about quantity and duration of oscillatory patterns for each of the 31 EEG channels and each of the 11 patients. We should note that the bioelectrical activity of the human brain in a state of nocturnal sleep demonstrates a characteristic monotonous dynamics. Moreover, the analysis of, for example, hypnogram polysomnography within a group does not allow distinguishing between different patients in the duration, number, or changes in sleep phases. Hence, we should note that the article is limited to the presentation of the data analysis method and this amount of patients is enough for method presentation. First of all, it was needed to find out some differences between healthy and illness patients. To simplify data analysis, we have calculated the averaged values of oscillatory patterns numbers and duration $T_{\Delta f_i}$ for each patient in 10 frequency intervals $\Delta f_i \; \forall \; i \in [1:10]$. Averaging was performed over all 31 EEG channels. These averaged oscillatory pattern lifetimes are depicted in Fig. 2. Red lines correspond to patients with MCI in group I (patients 1–6), whereas green lines correspond to group II (patients 7–11). Vertical axis represents averaged oscillatory pattern lifetime $T\Delta f_i$ in seconds; different panels were prepared for several frequency intervals Δf_i.

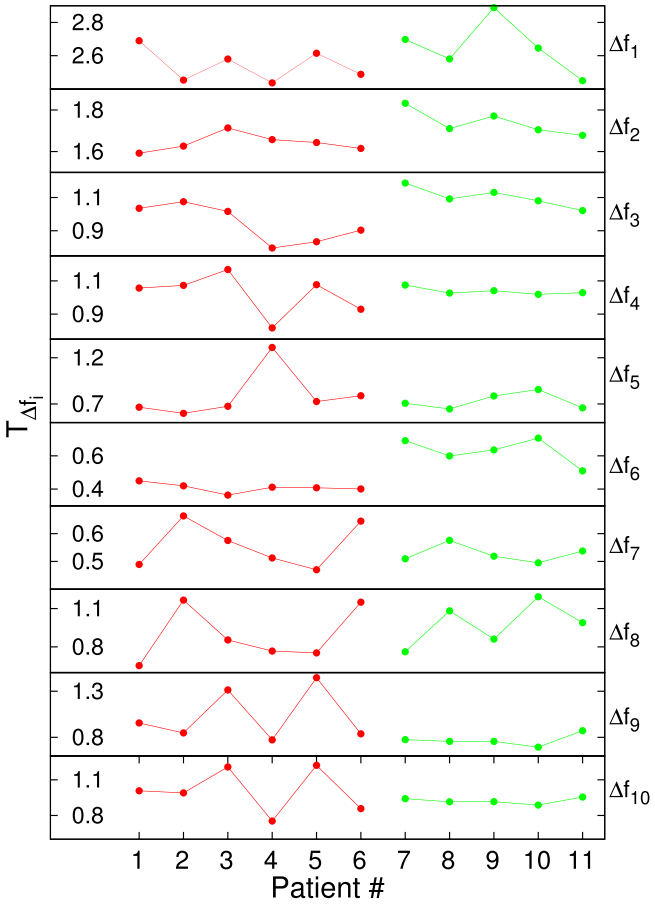

FIG. 2. Averaged oscillatory pattern lifetimes in seconds for patients with MCI (red lines) and healthy patients (green lines) for different frequency bands Δf_i.

The analysis of the number of oscillatory patterns does not show any differences between healthy and illness patients.

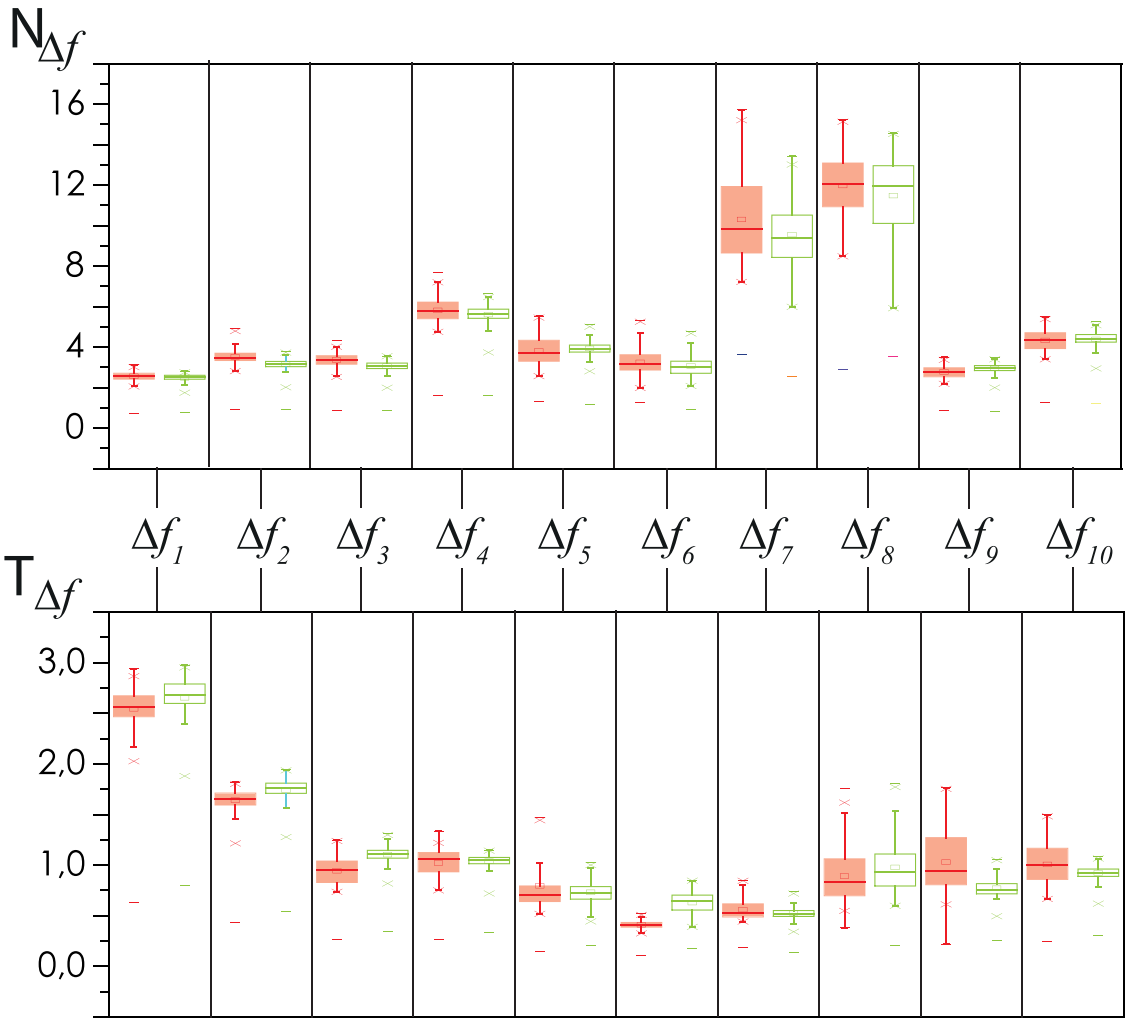

FIG. 3. Average number of patterns (top panel) and their average durations (bottom panel). For the patients of the first group, the diagrams are filled in red (gray in black and white), and the diagrams for the patients of the second group are inside white with a green outline.

Oscillatory patterns' lifetimes do not significantly differ in most of the frequency intervals too. But in Δf_2, Δf_3, and, to a greater extent, in Δf_6, the averaged duration of oscillatory patterns for healthy patients is longer than for illness ones.

Obviously, this qualitative observation requires a quantitative assessment. As such an estimate, it is reasonable to use statistical characteristics averaged over a set of illness and healthy patients. The statistical analysis of number and lifetimes of oscillatory patterns for all EEG channels is shown in Fig. 3. The top panel of Fig. 3 shows averaged quantity of patterns, whereas the bottom panel shows its averaged lifetime. This representation allows us to compare the number and duration of patterns in the same frequency range and is easily interpreted as follows. For example, Δf_1 is characterized by significant duration and a small number of patterns. It means that oscillations with frequencies in range [1:2.5] Hz observes rare but with significant duration. On the other hand for Δf_7, we can see that patterns observes most often with short duration. Drawing a parallel with Fig. 2, the notable differences in oscillatory patterns' averaged lifetimes become apparent for Δf_3 and Δf_6. However, the differences in lifetime for frequency interval Δf_3 are rather small, so they intersect within their interquartile ranges. Nevertheless, the panel with Δf_6 shows the intersection for only minimum and maximum sample values, whereas interquartile ranges are disjoint. Observed effects are realized both in hemispheres and on the midline [Figs. 4(a)–4(c)]. The statistical analysis based on the Wilcoxon test demonstrates significant differences in these characteristics for specified ranges, $p < 0.01$.

It should be noted separately that only the average lifetime of patterns differs but not their number (Fig. 3, top panel).

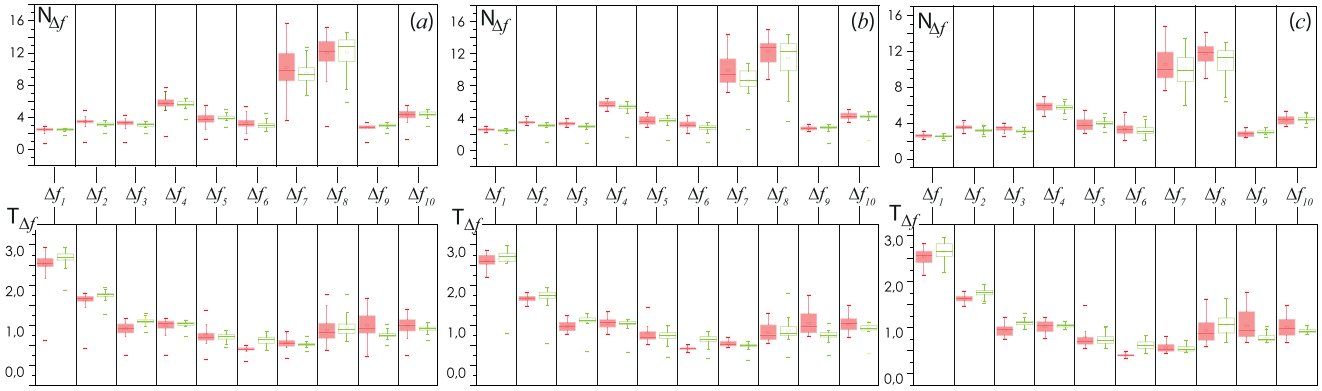

FIG. 4. Average number of patterns (top panels) and their average durations in seconds (bottom panels) for left hemisphere electrodes (a), center electrodes (b), and right hemisphere electrodes (c).

IV. DISCUSSION

Our study demonstrates that MCI causes changes in brain electrical activity in the frequency band $f \in [12; 14]$ Hz, which corresponds to the Beta rhythm (Beta 1 power). It is known from Refs. 62 and 63 that oscillations in the beta wave are interconnected with activity in the motor cortex. The primary and secondary motor and somatosensory cortex is located in the area of the central gyrus. Thus, the changes in the frequency range $\Delta f_6 \in [12; 14]$ Hz can be interpreted as related to the activity in the motor cortex.

To confirm this statement, let us consider the distribution of the lifetimes of patterns from this frequency range over the EEG electrodes, as shown in Fig. 5. The difference between lifetimes of oscillatory patterns of conditionally healthy and MCI patients is maximum in signals from electrodes FT7, C3, Cz, C4, CPz, and CP3. These electrodes were located in the left frontal and central regions of the scalp (see Fig. 1, electrodes with a squared green background). In other words, most of them are located directly above

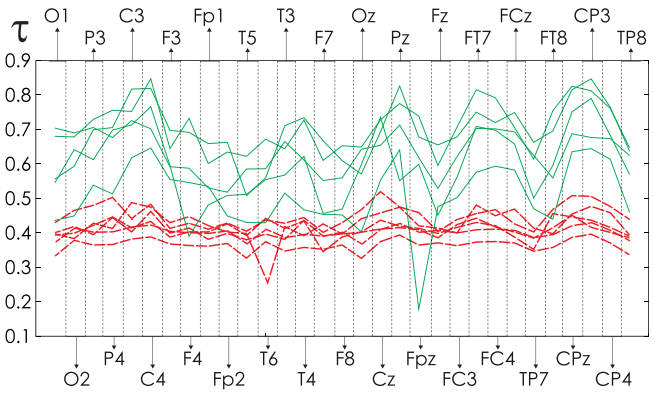

FIG. 5. Lifetimes in seconds of patterns for each of 31 EEG channels in frequency band Δf_6. Curves for group I are shown with red dashed lines. Difference between healthy and illness patients alter from channel to channel.

the brain regions of left temporal gyrus and central gyrus. Today, numerous studies link the impairments in the cognitive background of patients observed in various states to changes in the activity of the motor cortex. For example, on the basis of transcranial magnetic stimulation (TMS), a decrease in the association between the motor activity of the dominant hand and areas of the brain associated with speech functions has been shown.[64] Moreover, as demonstrated in Refs. 65–67, even mild cognitive decline is correlated with observed gait disorders, owing to probable changes in higher levels of motor control. In turn, MRI studies in case of gait disturbance demonstrated a decrease in the volume of some parts of the motor cortex of the brain. Thus, the revealed changes in the activity of the motor cortex during sleep supplement the already available information and emphasize that these variations persist in humans even during nighttime rest.

Such an uneven spatial change in the estimated characteristic of the oscillatory pattern's duration is probably associated with the well-known disturbance of global synchronization in classic alpha, beta, and gamma frequency bands.[68] In addition, it is known that MCI subjects with hippocampal atrophy have certain EEG activity changes, which showed the increase in the theta and alpha power on frontal and temporo-parietal areas.[69] Moreover, the obtained spatial distribution demonstrates the patterns of lateral nature corresponding to the described reductions in complexity and an increase in the predictability of EEG signals as in the review.[70] When analyzing the duration of oscillatory patterns observed in groups of patients with mild cognitive impairments, we observe a decrease in the frequency ranges, up to Δ_7, which corresponds to delta, theta, and alpha oscillatory modes. In other words, synchronous neural activity, leading to the emergence of oscillatory patterns in these frequency ranges, lasts at time intervals with a shorter length than in the groups of conventionally healthy subjects. From the point of view of the presented numerical approach to the assessment of EEG characteristics, we observe an extremely similar dynamics of the lifetime of oscillatory patterns in the scalp space (see Fig. 5). In other words, for MCI patients, we observe a significantly smaller spread in the duration of patterns in the EEG channels compared to the group of conventionally healthy participants. We assume that this can be interpreted as a

decrease in the complexity of oscillatory processes in the bioelectric activity of the brain.

The above results of assessing changes in EEG activity correlated with MCI-diagnosis have been obtained by a direct analysis of the entire nocturnal sleep recording. Polysomnographic separation at sleep stages is still difficult to analyze automatically and may involve some subjectivity on the part of the specialist somnologist.[71,72] A simple diagnostic approach based on the study and quantification of records of all night sleep appears to be quite interesting and promising.

ACKNOWLEDGMENTS

This work was supported by the RF Government under Grant No. 075-15-2019-1885 as part of collecting neurophysiological data. As a part of the clinical data interpretation, the study is carried out within the framework of the state task of the Russian Federation's Ministry of Health No. 056-00030-21-01 dated 02/05/2021 "Theoretical and experimental study of the integrative activity of various physiological systems of patient under stress" (the State Registration No. 121030900357-3).

DATA AVAILABILITY

The data that support the findings of this study are available from the corresponding author upon reasonable request.

REFERENCES

[1] A. Burns and S. Iliffe, "Alzheimers disease," BMJ **338**, b158–b158 (2009).
[2] A. Shimokawa, N. Yatomi, S. Anamizu, H. Torii, S. Isono, Y. Sugai, and M. Kohno, "Influence of deteriorating ability of emotional comprehension on interpersonal behavior in Alzheimer-type dementia," Brain Cognit. **47**, 423–433 (2001).
[3] J. Dauwels, F. Vialatte, and A. Cichocki, "Diagnosis of Alzheimer's disease from EEG signals: Where are we standing?," Curr. Alzheimer Res. **7**, 487–505 (2010).
[4] G. M. McKhann, D. S. Knopman, H. Chertkow, B. T. Hyman, C. R. Jack, Jr., C. H. Kawas, W. E. Klunk, W. J. Koroshetz, J. J. Manly, R. Mayeux *et al.*, "The diagnosis of dementia due to Alzheimer's disease: Recommendations from the National Institute on Aging-Alzheimer's Association workgroups on diagnostic guidelines for Alzheimer's disease," Alzheimers Dement. **7**, 263–269 (2011).
[5] V. L. Begali, "Neuropsychology and the dementia spectrum: Differential diagnosis, clinical management, and forensic utility," NeuroRehabilitation **46**, 181–194 (2020).
[6] B. Small, E. Gagnon, and B. Robinson, "Early identification of cognitive deficits: Preclinical Alzheimer's disease and mild cognitive impairment," Geriatrics **62**(4), 19–23 (2007).
[7] K. Palmer, A. Berger, R. Monastero, B. Winblad, L. Bäckman, and L. Fratiglioni, "Predictors of progression from mild cognitive impairment to Alzheimer disease," Neurology **68**, 1596–1602 (2007).
[8] E. Arnáiz and O. Almkvist, "Neuropsychological features of mild cognitive impairment and preclinical Alzheimer's disease," Acta Neurol. Scand. Suppl. **107**, 34–41 (2003).
[9] M. Weiner, "Imaging and biomarkers will be used for detection and monitoring progression of early Alzheimer's disease," J. Nutr. Health Aging **13**, 332 (2009).
[10] T. Sunderland, H. Hampel, M. Takeda, K. Putnam, and R. Cohen, "Biomarkers in the diagnosis of Alzheimer's disease: Are we ready?," J. Geriatr. Psychiatry Neurol. **19**, 172–179 (2006).
[11] H. Adeli, Z. Zhou, and N. Dadmehr, "Analysis of EEG records in an epileptic patient using wavelet transform," J. Neurosci. Methods **123**, 69–87 (2003).
[12] J. Britton, L. Frey, and J. Hopp, *Electroencephalography (EEG): An Introductory Text and Atlas of Normal and Abnormal Findings in Adults, Children, and Infants*, edited by E. St. Louis and L. Frey (American Epilepsy Society, Chicago, IL, 2016).
[13] J. Dauwels, F. Vialatte, T. Musha, and A. Cichocki, "A comparative study of synchrony measures for the early diagnosis of Alzheimer's disease based on EEG," NeuroImage **49**, 668–693 (2010).
[14] J. Jeong, "EEG dynamics in patients with Alzheimer's disease," Clin. Neurophysiol. **115**, 1490–1505 (2004).
[15] D. Tepas, "Computer analysis of the electroencephalogram: Evoking, promoting, and provoking," Behav. Res. Methods Instrum. **6**, 95–110 (1974).
[16] J. V. Odom, M. Bach, C. Barber, M. Brigell, M. F. Marmor, A. P. Tormene, G. E. Holder *et al.*, "Visual evoked potentials standard (2004)," Doc. Ophthalmol. **108**, 115–123 (2004).
[17] K. Bennys, F. Portet, J. Touchon, and G. Rondouin, "Diagnostic value of event-related evoked potentials n200 and p300 subcomponents in early diagnosis of Alzheimer's disease and mild cognitive impairment," J. Clin. Neurophysiol. **24**, 405–412 (2007).
[18] D. A. Kaiser, "Basic principles of quantitative EEG," J. Adult Dev. **12**, 99–104 (2005).
[19] P. Singh and R. B. Pachori, "Classification of focal and nonfocal EEG signals using features derived from Fourier-based rhythms," J. Mech. Med. Biol. **17**, 1740002 (2017).
[20] G. Chen, G. Lu, W. Shang, and Z. Xie, "Automated change-point detection of EEG signals based on structural time-series analysis," IEEE Access **7**, 180168–180180 (2019).
[21] A. M. Maitín, R. Perezzan, D. Herráez-Aguilar, J. I. Serrano, M. D. Del Castillo, A. Arroyo, J. Andreo, and J. P. R. Muñoz, "Time series analysis applied to EEG shows increased global connectivity during motor activation detected in pd patients compared to controls," Appl. Sci. **11**, 15 (2021).
[22] B. Weiss, Z. Clemens, R. Bódizs, Z. Vágó, and P. Halász, "Spatio-temporal analysis of monofractal and multifractal properties of the human sleep EEG," J. Neurosci. Methods **185**, 116–124 (2009).
[23] J. Yan, S. L. Risacher, L. Shen, and A. J. Saykin, "Network approaches to systems biology analysis of complex disease: Integrative methods for multi-omics data," Brief. Bioinf. **19**, 1370–1381 (2018).
[24] J. Mateo, A. Torres, M. A. García, and J. Santos, "Noise removal in electroencephalogram signals using an artificial neural network based on the simultaneous perturbation method," Neural Comput. Appl. **27**, 1941–1957 (2016).
[25] T. Radüntz, J. Scouten, O. Hochmuth, and B. Meffert, "Automated EEG artifact elimination by applying machine learning algorithms to ICA-based features," J. Neural Eng. **14**, 046004 (2017).
[26] E. M. Ventouras, E. A. Monoyiou, P. Y. Ktonas, T. Paparrigopoulos, D. G. Dikeos, N. K. Uzunoglu, and C. R. Soldatos, "Sleep spindle detection using artificial neural networks trained with filtered time-domain EEG: A feasibility study," Comput. Methods Programs Biomed. **78**, 191–207 (2005).
[27] N. Kasabov and E. Capecci, "Spiking neural network methodology for modelling, classification and understanding of EEG spatio-temporal data measuring cognitive processes," Inf. Sci. **294**, 565–575 (2015).
[28] R. Tripathy and U. R. Acharya, "Use of features from rr-time series and EEG signals for automated classification of sleep stages in deep neural network framework," Biocybern. Biomed. Eng. **38**, 890–902 (2018).
[29] J. Cho and H. Hwang, "Spatio-temporal representation of an electoencephalogram for emotion recognition using a three-dimensional convolutional neural network," Sensors **20**, 3491 (2020).
[30] B. O. Peters, G. Pfurtscheller, and H. Flyvbjerg, "Mining multi-channel EEG for its information content: An ANN-based method for a brain–computer interface," Neural Netw. **11**, 1429–1433 (1998).
[31] H. Ghonchi, M. Fateh, V. Abolghasemi, S. Ferdowsi, and M. Rezvani, "Spatio-temporal deep learning for EEG-fNIRS brain computer interface," in *2020 42nd Annual International Conference of the IEEE Engineering in Medicine & Biology Society (EMBC)* (IEEE, 2020), pp. 124–127.
[32] A. N. Pavlov, N. B. Janson, V. S. Anishchenko, V. I. Gridnev, and P. Y. Dovgalevsky, "Diagnostic of cardio-vascular disease with help of largest Lyapunov exponent of rr-sequences," Chaos Solitons Fractals **11**, 807–814 (2000).
[33] V. A. Maksimenko, A. Pavlov, A. E. Runnova, V. Nedaivozov, V. Grubov, A. Koronovslii, S. V. Pchelintseva, E. Pitsik, A. N. Pisarchik, and A. E. Hramov,

"Nonlinear analysis of brain activity, associated with motor action and motor imaginary in untrained subjects," Nonlinear Dyn. **91**, 2803–2817 (2018).
[34]V. S. Anishchenko, A. G. Balanov, N. B. Janson, N. B. Igosheva, and G. V. Bordyugov, "Synchronization of heart rate by sound and light pulses," AIP Conf. Proc. **502**, 162–167 (2000).
[35]V. S. Anishchenko, A. G. Balanov, N. B. Janson, N. B. Igosheva, and G. V. Bordyugov, "Synchronization of cardiorhythm by weak external forcing," Discrete Dyn. Nat. Soc. **4**, 139439 (2000).
[36]N. Janson, A. Balanov, V. S. Anishchenko, and P. McClintock, "Phase relationships between two or more interacting processes from one-dimensional time series. II. Application to heart-rate-variability data," Phys. Rev. E **65**, 036212 (2002).
[37]V. S. Anishchenko, N. B. Igosheva, A. Pavlov, A. Khovanov, and T. Yakusheva, "Comparative analysis of methods for classifying the cardiovascular system's states under stress," Crit. Rev. Biomed. Eng. **29**, 462–481 (2001).
[38]V. S. Anishchenko, A. Balanov, N. B. Janson, N. B. Igosheva, and G. V. Bordyugov, "Entrainment between heart rate and weak noninvasive forcing," Int. J. Bifurcation Chaos **10**, 2339–2348 (2000).
[39]V. S. Anishchenko, N. B. Yanson, and A. Pavlov, "Work of the human heart: A regular process?," J. Commun. Technol. Electron. **42**(8), 936–940 (1997).
[40]N. B. Igosheva, N. B. Janson, A. G. Balanov, T. P. Romanova, O. V. Glushkovskaja-Semjachkina, T. G. Anishchenko, and V. S. Anishchenko, "Dynamics of blood pressure in healthy rats at rest and after stress," AIP Conf. Proc. **502**, 168–174 (2000).
[41]M. Unser and A. Aldroubi, "A review of wavelets in biomedical applications," Proc. IEEE **84**, 626–638 (1996).
[42]T. Nguyen, A. Khosravi, D. Creighton, and S. Nahavandi, "EEG signal classification for bci applications by wavelets and interval type-2 fuzzy logic systems," Expert Syst. Appl. **42**, 4370–4380 (2015).
[43]N. Semenova, K. Segreev, A. Slepnev, A. Runnova, M. Zhuravlev, I. Blokhina, A. Dubrovsky, O. Semyachkina-Glushkovskaya, and J. Kurths, "Non-invasive analysis of blood-brain barrier permeability based on wavelet and machine learning approaches," arXiv:2103.05693 (2021).
[44]K. Tzimourta, A. Tzallas, N. Giannakeas, L. Astrakas, D. Tsalikakis, and M. Tsipouras, "Epileptic seizures classification based on long-term EEG signal wavelet analysis," in *International Conference on Biomedical and Health Informatics* (Springer, 2017), pp. 165–169.
[45]V. Grubov, E. Sitnikova, A. Pavlov, A. Koronovskii, and A. Hramov, "Recognizing of stereotypic patterns in epileptic EEG using empirical modes and wavelets," Physica A **486**, 206–217 (2017).
[46]R. Tripathy, S. Ghosh, P. Gajbhiye, and U. Acharya, "Development of automated sleep stage classification system using multivariate projection-based fixed boundary empirical wavelet transform and entropy features extracted from multichannel EEG signals," Entropy **22**, 1141 (2020).
[47]V. Bajaj and R. Pachori, "Automatic classification of sleep stages based on the time-frequency image of EEG signals," Comput. Methods Programs Biomed. **112**, 320–328 (2013).
[48]E. C. Djamal and R. D. Putra, "Brain-computer interface of focus and motor imagery using wavelet and recurrent neural networks," TELKOMNIKA Telecommun. Comput. Electron. Control **18**, 2748–2756 (2020).
[49]I. T. Hettiarachchi, T. T. Nguyen, and S. Nahavandi, "Motor imagery data classification for bci application using wavelet packet feature extraction," in *International Conference on Neural Information Processing* (Springer, 2014), pp. 519–526.
[50]Z. S. Nasreddine, N. A. Phillips, V. Bédirian, S. Charbonneau, V. Whitehead, I. Collin, J. L. Cummings, and H. Chertkow, "The montreal cognitive assessment, moca: A brief screening tool for mild cognitive impairment," J. Am. Geriatr. Soc. **53**, 695–699 (2005).
[51]G. Klem, H. Lüders, H. Jasper, and C. Elger, "The ten-twenty electrode system of the international federation. The international federation of clinical neurophysiology," Electroencephalogr. Clin. Neurophysiol. Suppl. **52**, 3–6 (1999).
[52]B. Torresani, "Continuous wavelet transform," Savoire Paris **675**, 676 (1995).
[53]A. E. Hramov, A. A. Koronovskii, V. A. Makarov, A. N. Pavlov, and E. Sitnikova, *Wavelets in Neuroscience* (Springer, 2015).
[54]A. N. Pavlov, A. E. Hramov, A. A. Koronovskii, E. Y. Sitnikova, V. A. Makarov, and A. A. Ovchinnikov, "Wavelet analysis in neurodynamics," Phys. Usp. **55**, 845 (2012).
[55]Z. Dai, J. De Souza, J. Lim, P. M. Ho, Y. Chen, J. Li, N. Thakor, A. Bezerianos, and Y. Sun, "EEG cortical connectivity analysis of working memory reveals topological reorganization in theta and alpha bands," Front. Hum. Neurosci. **11**, 237 (2017).
[56]U. Braun, A. Schäfer, H. Walter, S. Erk, N. Romanczuk-Seiferth, L. Haddad, J. I. Schweiger, O. Grimm, A. Heinz, H. Tost *et al.*, "Dynamic reconfiguration of frontal brain networks during executive cognition in humans," Proc. Natl. Acad. Sci. U.S.A. **112**, 11678–11683 (2015).
[57]V. V. Makarov, M. O. Zhuravlev, A. E. Runnova, P. Protasov, V. A. Maksimenko, N. S. Frolov, A. N. Pisarchik, and A. E. Hramov, "Betweenness centrality in multiplex brain network during mental task evaluation," Phys. Rev. E **98**, 062413 (2018).
[58]N. Semenova and A. Zakharova, "Weak multiplexing induces coherence resonance," Chaos **28**, 051104 (2018).
[59]E. Sitnikova, A. E. Hramov, V. Grubov, and A. A. Koronovsky, "Age-dependent increase of absence seizures and intrinsic frequency dynamics of sleep spindles in rats," Neurosci. J. **2014**, 370764.
[60]E. Sitnikova, A. E. Hramov, V. Grubov, and A. A. Koronovsky, "Time-frequency characteristics and dynamics of sleep spindles in WAG/Rij rats with absence epilepsy," Brain Res. **1543**, 290–299 (2014).
[61]J. J. Newson and T. C. Thiagarajan, "EEG frequency bands in psychiatric disorders: A review of resting state studies," Front. Hum. Neurosci. **12**, 521 (2019).
[62]R. Hari and R. Salmelin, "Human cortical oscillations: A neuromagnetic view through the skull," Trends Neurosci. **20**, 44–49 (1997).
[63]O. Jensen, P. Goel, N. Kopell, M. Pohja, R. Hari, and B. Ermentrout, "On the human sensorimotor-cortex beta rhythm: Sources and modeling," Neuroimage **26**, 347–355 (2005).
[64]L. Bracco, F. Giovannelli, V. Bessi, A. Borgheresi, A. Di Tullio, S. Sorbi, G. Zaccara, and M. Cincotta, "Mild cognitive impairment: Loss of linguistic task-induced changes in motor cortex excitability," Neurology **72**, 928–934 (2009).
[65]C. Annweiler, O. Beauchet, R. Bartha, J. L. Wells, M. J. Borrie, V. Hachinski, and M. Montero-Odasso, "Motor cortex and gait in mild cognitive impairment: A magnetic resonance spectroscopy and volumetric imaging study," Brain **136**, 859–871 (2013).
[66]C. Annweiler, O. Beauchet, S. Celle, F. Roche, T. Annweiler, G. Allali, R. Bartha, and M. Montero-Odasso, "Contribution of brain imaging to the understanding of gait disorders in Alzheimer's disease: A systematic review," Am. J. Alzheimers Dis. Other Demen. **27**, 371–380 (2012).
[67]Å. von Berens, A. Koochek, M. Nydahl, R. Fielding, T. Gustafsson, D. Kirn, T. Cederholm, and M. Södergren, "'Feeling more self-confident, cheerful and safe.' Experiences from a health-promoting intervention in community dwelling older adults—A qualitative study," J. Nutr. Health Aging **22**, 541–548 (2018).
[68]T. König, L. Prichep, T. Dierks, D. Hubl, L. Wahlund, E. John, and V. Jelic, "Decreased EEG synchronization in Alzheimer's disease and mild cognitive impairment," Neurobiol. Aging **26**, 165–171 (2005).
[69]C. Babiloni, G. B. Frisoni, M. Pievani, F. Vecchio, R. Lizio, M. Buttiglione, C. Geroldi, C. Fracassi, F. Eusebi, R. Ferri *et al.*, "Hippocampal volume and cortical sources of EEG alpha rhythms in mild cognitive impairment and Alzheimer disease," Neuroimage **44**, 123–135 (2009).
[70]J. Sun, B. Wang, Y. Niu, Y. Tan, C. Fan, N. Zhang, J. Xue, J. Wei, and J. Xiang, "Complexity analysis of EEG, MEG, and FMRI in mild cognitive impairment and Alzheimer's disease: A review," Entropy **22**, 239 (2020).
[71]M. Cesari, A. Stefani, T. Penzel, A. Ibrahim, H. Hackner, A. Heidbreder, A. Szentkirályi, B. Stubbe, H. Völzke, K. Berger *et al.*, "Inter-rater sleep stage scoring reliability between manual scoring from two European sleep centers and automatic scoring performed by the artificial intelligence-based stanford-stages algorithm," J. Clin. Sleep Med. **17**, 1237–1247 (2021).
[72]J. Vanbuis, M. Feuilloy, G. Baffet, N. Meslier, F. Gagnadoux, and J.-M. Girault, "Towards a user-friendly sleep staging system for polysomnography part I: Automatic classification based on medical knowledge," Inf. Med. Unlocked **21**, 100454 (2020).